Materials Science & Engineering A 699 (2017) 71–80

Contents lists available at ScienceDirect

Materials Science & Engineering A

journal homepage: www.elsevier.com/locate/msea

Microstructure and texture evolution of TA32 titanium alloy during superplastic deformation

Zhangguang Liu[a,b,*], Peijie Li[a], Linlin Geng[c], Taiying Liu[b], Haitao gao[b]

[a] National Center of Novel Materials for International Research, Tsinghua University, Beijing 100084, China
[b] Beijing Xinghang Electro-mechanical Equipment Co., Ltd., Beijing 100074, China
[c] Beijing North Vehicle Group Corporation, Beijing 100072, China

ARTICLE INFO

Keywords:
Dynamic recrystallization
EBSD
Grain boundaries
Textures
Microstructures

ABSTRACT

A study based on uniaxial tension tests were conducted in this paper to understand the hot deformation behaviors of TA32 alloy during superplastic deformation at a deformation temperature of 915 °C and an initial strain rate of $6.64 \times 10^{-3}\ s^{-1}$. In the test, the maximum fracture elongation reached 1065%, exhibiting good superplastic deformation ability. Electron back-scattered diffraction (EBSD) was used to analyze and study evolution of microstructures and textures in the process of deformation with the following findings: During tensile deformation, the fraction of low-angle grain boundaries (< 15 °, LAGBs) decreased drastically, while that of high-angle grain boundaries (≥15 °, HAGBs) increased from 45% to 96.2%. As the further straining, the role of continuous dynamic recrystallization (CDRX) was weakened, while that of discontinuous dynamic recrystallization (DDRX) was strengthened. Dynamic recrystallization helped refine coarse grains in the initial structures and reduced deformation defects in grains. The superplastic deformation mechanism of TA32 alloy was dominated by boundary sliding of high-angle grains, coordinated by dislocation motion at the softening stage and by grain rotation at the steady deformation stage respectively. In addition, the drawing force contributed to both dynamic recrystallization and rotation of grains.

1. Introduction

In the researches and development of ultrasonic cruise missiles, hypersonic cruise missiles, reusable vehicles, and sub-orbital reusable trans-atmospheric vehicles, titanium alloy has to be operated at high temperatures (even 650 °C), due to which an excellent temperature resistance is required. Development of titanium alloy for high temperature applications, though extremely active and important, has been quite strenuous. This is mainly because requirements for such alloy, including good room-temperature property, high-temperature strength, creep performance, thermal stability, fatigue behavior, and facture toughness, can't be met easily at the same time [1,2], and they often lead to contradictory needs for material composition and structure. Some high-temperature titanium alloys such as IM829 [3], IMI834 [4], BT36 [5], Ti-1100 [6], Ti60 [7] and Ti600 [8] have been successfully developed to meet loading requirements in high temperature applications. In recent years, Institute of Metal Research, Chinese Academy of Sciences designed a near-α type heat-resistant high temperature alloy with the nominal chemical composition of Ti-5Al-4Sn-2Zr-1Mo-0.25Si-1Nd (wt%). Addition of a small amount of rare earth element Nd provided it with both good heat resistance and good thermal stability 550 °C [9–11]. In spite of favorable casting and plastic forming performance [12], this alloy has an suboptimal welding property due to presence of rare earth element Nd. Welded parts of such alloy are more likely to crack and difficult to be used widely in engineering applications. To address this, Institute of Metal Research, Chinese Academy of Sciences optimized its composition by eliminating rare earth element Nd and added heat-resistant elements Ta and Nb. In this way, the alloy achieved greatly improved weldability while keeping heat resistance and thermal stability. It was renamed as TA32 [13].

TA32 alloy is a new near-α titanium alloy with a nominal chemical composition of Ti-5.2 Al-3.5Sn-3.0Zr-1.0Mo-0.4Ta-0.4 Nb-0.25Si (wt %). It features quite a few of chemical constituents, low content of β-stability elements, inferior process plasticity, leading to a narrow range of temperature for plastic forming. For thin-walled production of TA32 alloy, superplastic forming serves as an effective means to overcome the poor formability of TA32 alloy at room temperature. The materials used for superplastic process should have fine equiaxial structures (typically not exceeding 10 μm) and should remain stable in the whole deformation range. The superplastic behaviors of materials were intrinsically

* Corresponding author at: National Center of Novel Materials for International Research, Tsinghua University, Beijing 100084, China.
E-mail address: liuzg13@mails.tsinghua.edu.cn (Z. Liu).

http://dx.doi.org/10.1016/j.msea.2017.05.082
Received 9 April 2017; Received in revised form 19 May 2017; Accepted 20 May 2017
Available online 22 May 2017
0921-5093/

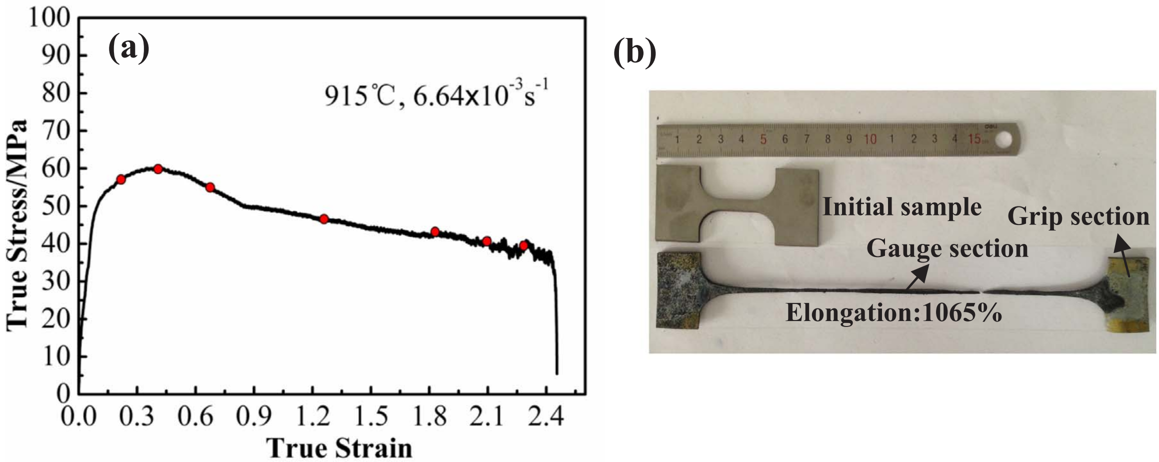

Fig. 1. True stress-strain curve of TA32 at 915 °C and 6.64 × 10^{-3} s^{-1}.

related to their microstructures [14–17], and changes of microstructures during superplastic deformation can influence mechanical behaviors and deformation mechanisms [18–22]. It is therefore necessary to study microstructure changes and deformation mechanisms during superplastic deformation. In recent years, researches on superplastic deformation behaviors of near-α high-temperature titanium alloy have gradually increased [12,23–25], and the microstructure changes and deformation mechanisms of a number of high-temperature titanium alloys during deformation have been studied [7,26–29], promoting the development of forming theory and process of such high-temperature alloys. However, currently there are few reports about microstructural evolution, textural changes, and deformation mechanisms of TA32 alloy sheets during superplastic tensile deformation. To better understand superplastic deformation behaviors of TA32 alloy, it is necessary to perform an in-depth study on microstructural evolution, textural changes, and deformation mechanisms of TA32 alloy during superplastic tensile deformation.

In this study, TA32 alloy was tested at a deformation temperature of 915 °C and an initial strain rate of 6.64 × 10^{-3} s^{-1}. EBSD technique was used to observe microstructural evolution and textural changes during superplastic deformation. The evolution process of grain boundaries, crystal orientations, and micro-textures were analyzed, followed by a discussion on superplastic deformation and recrystallization mechanisms of TA32 alloy. This study was intended to provide experimental basis and theoretical guidance for superplastic forming process of TA32 alloy sheets, and to speed up industrial application of such advanced material.

2. Experiments

The materials used for tests were hot rolled and annealed TA32 alloy sheet 2.0 mm in thickness provided by Baoti Group, with a measured chemical composition of Ti-5.3Al-3.5Sn-3.0Zr-1.0Mo-0.4Ta-0.5 Nb-0.25Si. The transformation temperature measured with metallographic method is about 1005 °C. All tension tests in this study were carried out on an Instron5500R tester. The test materials were drawn along the rolling direction and the size of gauge section was 15 mm × 5 mm × 2 mm. The samples were then polished with SiC waterproof abrasive paper to eliminate any transverse scratches on all sample surfaces in the standard gauge length area. High-temperature anti-oxidation coatings were applied to the sample surface prior to test to avoid oxidation during tension. The samples were heated in a furnace to the predefined temperature and remained the given temperature for 10 min before tension. The tension deformation temperature was selected as 915 °C. During the tension test, the speed of the clamp head was fixed at a constant level corresponding to an initial strain rate of 6.64 × 10^{-3} s^{-1} and the fracture elongation was 1065%, representing the corresponding true strain value of 2.46. To better study microstructure changes and textural evolution during tensile deformation, the tension force was withdrawn immediately whenever a specified true strain value is reached. The true strain values were 0.15, 0.35, 0.65, 1.25, 1.80, 2.14, and 2.30 respectively, which covered all major deformation stages and areas in the tensile deformation conditions of 915 °C and 6.64 × 10^{-3} s^{-1}. The samples were taken out immediately after deformation and quenched with water to preserve microstructures. The orientation analysis was studied by EBSD technique. The EBSD scan surface is the rolling surface (RD-TD). The scan step and approximate scan area were 0.6 µm and 110 µm × 110 µm respectively. The EBSD measurement results were analyzed with TSL OIM 6.1.3 software. In order to minimize the impact of noise, the minimum confidence index was set 0.2.

The grain boundary distribution maps show the fractions and distribution of high-angle grain boundaries (HAGBs) and low-angle grain boundaries (LAGBs). In this study, HAGBs correspond to misorientation angles higher than 15°, while LAGBs correspond to 2–15°. Inverse pole figures (IPF) show grain orientation parallel to normal direction of rolling sheet. Image quality (IQ) maps are related to defects in the crystals. A higher IQ value indicates a lower number of crystal defects. This value can be used as an index of grain recovery and dynamic recrystallization degree [30]. Grains orientation spread (GOS) maps reveal plastic strain characteristics of crystals. In general, grain deformation will cause defects in grains. The more defects, the higher GOS value. Conversely, defect-free grains that have not experienced deformation have the lower GOS value [31]. Statistical distribution of GOS can be used for quantitative analysis of misorientation angles in grains, while grain misorientation angle statistics show statistical distribution of misorientation angles between neighboring grains.

3. Results and discussion

3.1. *True stress–strain curve*

The true stress-strain curve of TA32 titanium alloy at 915 °C and 6.64 × 10^{-3} s^{-1} is shown in Fig. 1. In the initial deformation stage, due to the high work hardening rate, the peak stress was reached at a very low strain and maintained for a short time before dropping rapidly. The steady deformation stage started when the stress dropped to 45 MPa. In this stage, the flow stress dropped slowly until tension fracture. In sum, the flow stress curves can be divided into three stages: In the initial deformation stage, the flow stress increased rapidly, and 60 MPa peak stress was reached at a strain of 0.35. This stage was dominated by work hardening. The second stage was characterized by